JOURNAL OF MATERIALS SCIENCE LETTERS 13 (1994) 573–576

An a.c. impedance study of LiI–Al_2O_3 composite solid electrolyte

J. S. BAE, S.-I. PYUN
Department of Materials Science and Engineering, Korea Advanced Institute of Science and Technology, 313 Kusung Dong, Yusung Gu, Daejon 305-701, Korea

It has been reported that the incorporation of insulating oxides such as Al_2O_3 and SiO_2 increases the cationic conductivity of anhydrous polycrystalline lithium iodide [1, 2]. Jow and Wagner [3] suggested that the enhanced cationic conductivity by addition of Al_2O_3 particles is due to the formation of a higher conductive interface region between matrix and oxide particles. Furthermore, lithium iodide is so extremely hygroscopic that it readily forms various hydrate phases under even a very low vapour pressure of waer (0.5 ppm v H_2O at 298 K). The presence of the hydrates favourably or detrimentally affects the ionic conductivities of lithium iodide–oxide composites actually used as solid electrolytes [4, 5].

Impedance spectroscopy [6] is known to be a useful method for making a distinction between conductive regions with different conductivities in an ionic solid. Depending upon the geometric arrangement of the various phases and the relative magnitude of their conductivities and dielectric constants, each phase can manifest itself by the presence of its own arc in an impedance plot. Although several studies [7, 8] have been conducted on LiI–Al_2O_3 composites by means of the measurement of a.c. conductivity simply at 1 kHz and of d.c. four-probe conductivity, they did not take into account the frequency dispersion of a.c. conductivity due to hydrate or interface region between LiI and Al_2O_3. Therefore, a detailed a.c. impedance analysis is still needed over a wide frequency range.

The present work is aimed at searching for a possible high conductive region within LiI–Al_2O_3 composites at 298–400 K and investigating the effect of crystal water remaining within LiI–Al_2O_3 composites on lithium ion conduction through LiI–Al_2O_3 composites. For this purpose, a.c. impedance measurements were performed at various temperatures and the measured impedance data were analysed using the complex non-linear least-squares (CNLS) fitting method [9].

Anhydrous lithium iodide (Foote Mineral Co., USA, purity 99.99%) and α-Al_2O_3 (High Purity Chemical Co., Japan, purity 99.9%, particle size 0.3 μm) powders were used as received without any pre-treatment. Anhydrous lithium iodide and undried Al_2O_3 powders were sufficiently well mixed in agate mortar and pestle. They were heated in an alumina crucible at 750 ± 30 K for 15–17 h, followed by quenching to room temperature. The LiI–Al_2O_3 composite chunk was finally pulverized and then pressed in a steel die under 850 MPa into disc specimens of the LiI 5, 10 and 20 mol % Al_2O_3 composites with diameter 1 cm and thickness 0.04–0.05 cm.

For impedance measurements, lithium electrodes were attached to both sides of the disc specimen. Two-probe impedance measurement was performed at various temperatures during the heating cycle from 314 to 400 K and the cooling cycle from 400 to 314 K, over a frequency range of 10^2 to 10^6 Hz using a Solartron high frequency response analyser (FRA) (Model SI 1255). Measured impedance data were corrected with values (1 MΩ and 35 pF) of input impedance of the FRA.

The disc specimen was maintained for 20 min at the measuring temperature prior to impedance measurement in order to assure the establishment of thermal equilibrium. Both the disc specimen preparation and the impedance measurement were carried out in a glove box (VAC HE 493) filled with purified argon gas in order to prevent the very reactive lithium and extremely hygroscopic lithium iodide from coming into contact with air. The content of H_2O vapour in the argon atmosphere of the glove box was monitored using phosphorus pentoxide (P_2O_5; 0.04 ppm v H_2O at 298 K) powder. Thus, we may assume that the atmospheric water vapour pressure was sufficiently below the critical value of 0.5 ppm v H_2O necessary for the formation of the lithium iodide hydrates.

The impedance plots of Z' against Z'', measured at 298 K for LiI containing various contents of Al_2O_3, are shown in Fig. 1. The magnitude of the arc decreased with increasing Al_2O_3 content. Since the

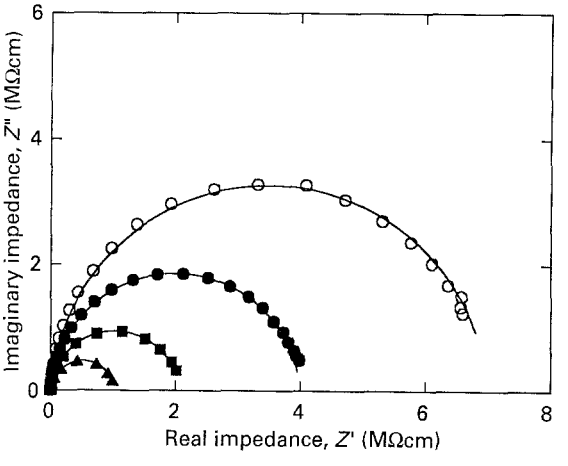

Figure 1 Impedance plots of Z' against Z'' obtained at 298 K from LiI containing various Al_2O_3 contents: (○), pure LiI; (●), 5 mol % Al_2O_3; (■), 10 mol % Al_2O_3; (▲), 20 mol % Al_2O_3.

faradaic reaction ($Li^+ + e^- = Li$) is known to proceed faster at the interface between LiI–Al_2O_3 composite electrolyte and lithium metal electrode, as compared to lithium ion transport through the LiI–Al_2O_3 composite [8], the arc can be attributed to LiI–Al_2O_3 bulk ion. As the content of incorporated Al_2O_3 increases from 0 to 20 mol %, the ionic conductivity of LiI–Al_2O_3 composites rises from 1.4×10^{-7} to 1.0×10^{-6} Ω^{-1} cm^{-1}.

It should be noted that only a single arc appears on complex plane over the whole frequency range investigated, regardless of Al_2O_3 content. LiI–Al_2O_3 composite is composed of LiI matrix, dispersed insulating Al_2O_3 particles and the interface region between LiI matrix and Al_2O_3 particles. If the dispersed Al_2O_3 particles are sufficiently separated from one another, the higher conductive interface region would be encompassed by the lower conductive lithium iodide matrix. In this case, the lithium ion conduction would occur through both the higher conductive interface region parallel to the direction of lithium ion conduction and the lower conductive lithium iodide matrix. Consequently, an additional arc assigned to the higher conductive interface should result in a complex impedance plane.

The percolation model combined with the effective medium model [9] on ionic conduction through a composite AB gives the percolation limit value of 10–15 vol % B, above which the continuous conduction path is provided. However, we did not actually observe any additional arc even at 5 mol % (3.4 vol %) Al_2O_3 content, which is much lower than the percolation limit. Therefore, it is strongly inferred that the enhanced lithium ion conductivity is not due to the higher conductive phase newly formed at the interface between LiI matrix and Al_2O_3 particle, but to lithium ion vacancy concentration in the lithium iodide matrix near Al_2O_3 particles.

Fig. 2 shows typical impedance spectra obtained from LiI-20 mol % Al_2O_3 composite during the heating and cooling cycles. During the heating cycle, a single arc results over the whole frequency range investigated, whereas during the cooling cycle, seriously depressed and merged arcs appear. Similar results were also observed for the other composite specimens (LiI 5 and 10 mol % Al_2O_3).

For analysis of the seriously depressed and merged impedance arcs, the CNLS fitting method [10] was employed. The equation for the total measured impedance spectra is:

$$Z_t = \frac{R_1}{1 + (j\omega R_1 C_1)^{\gamma_1}} + \frac{R_2}{1 + (j\omega R_2 C_2)^{\gamma_2}}, \quad j = -1^{1/2} \tag{1}$$

where ω is angular frequency, R_i and C_i represent resistance and capacitance for an arc on the complex impedance plane and the distribution parameter γ_1 in the equivalent circuit was introduced to quantify the dispersion of impedance spectral data. The first and second terms of Equation 1 correspond to the high and low frequency arcs, respectively. The

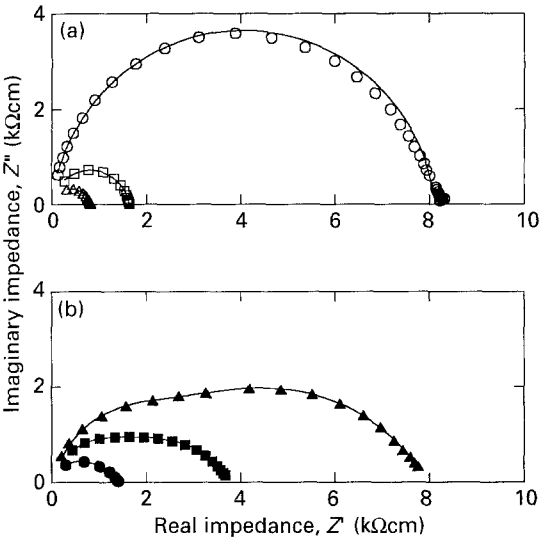

Figure 2 Typical impedance plots of Z' against Z'' obtained from LiI containing 20 mol % Al_2O_3 during (a) the heating cycle, measured at temperatures of: (○), 328 K; (□), 360 K; (△), 382 K; and (b) during the cooling cycle, measured at temperatures of: (●), 390 K, (■), 371 K; (▲), 358 K. The cooling cycle runs were preceded by holding the specimen at 400 K for 1 h.

parameters R_i, C_i and γ_1 in Equation 1 were determined by fitting the measured impedance data so that weighted sums (S) of squared residuals were minimized:

$$S = \sum_i^n \left(\frac{(Z'_{ei} - Z'_{ti})^2}{|Z'_{ei}|^2} + \frac{(Z''_{ei} - Z''_{ti})^2}{|Z''_{ei}|^2} \right) \tag{2}$$

where Z'_{ei} and Z''_{ei} are the real and imaginary parts of measured impedance data and Z'_{t_i} and Z''_{t_i} are the real and imaginary impedances theoretically calculated from Equation 1. The standard deviations S_k of each estimated parameter R_i, C_i and γ_i were calculated from the formula proposed by Walter *et al.* [11], given by:

$$S_k = \left[\left(\frac{S}{2N - M} \right) H_{kk}^{-1} \right]^{1/2} \tag{3}$$

where S is a weighted sum of squared residuals, N is the number of measured impedance data, M is the number of circuit parameters, and H_{kk} is the (k, k)th component of the Hessian matrix ($2J^TJ$; J = Jacobian matrix). The values of standard deviations S_k for the estimated parameters were calculated to be 0.01 to 1.2%, suggesting the validity of those parameters. The computer code used in data fitting was developed recently in our laboratory.

The results of fitting are given in Table I. The values of capacitance C_i and relaxation time distribution parameter γ_i were not considerably changed with decreasing temperature. The overall shape change of impedance spectra was mainly determined by resistance elements R_i. The parameter γ_2 (0.66 to 0.78) obtained from the low frequency arc was relatively low, as compared to the values (0.91 to 0.98) from the high frequency arc. According to Cole and Cole [12], the value of γ is closely related to the distribution of relaxation time for charge transport. In other words, as the value of

TABLE I Fit parameters for impedance data obtained from LiI-20 mol % Al_2O_3 composite at various temperatures during the cooling cycle, using the CNLS fitting method. Specimen thickness (d) = 0.05 cm, area (A) = 0.785 cm^2

T (K)	σ_1^a ($\mu\Omega^{-1}$ cm^{-1})	C_1 (nF)	γ_1	σ_2^a ($\mu\Omega^{-1}$ cm^{-1})	C_2 (nF)	γ_2
390	92	0.48	0.91	15	1.4	0.66
371	47	0.47	0.94	4.8	2.0	0.68
358	28	0.48	0.97	2.1	2.2	0.70
331	5.4	0.47	0.96	2.3	2.2	0.77
321	4.0	0.47	0.98	0.15	2.2	0.78
314	3.0	0.50	0.98	0.09	2.0	0.78
298[b]	1.0			0.02		

[a]The thickness (d_1, d_2) of the respective phases responsible for the two arcs were determined from the relations, $d_1/d_2 = (\varepsilon_1 C_2)/(\varepsilon_2 C_1)$ (ε_1 is the relative dielectric constant) and $d = d_1 + d_2$, assuming that $\varepsilon_1 \approx \varepsilon_2$.

[b]Calculated from the $\sigma = \sigma_0/T \exp[-E_a/RT]$ (σ is ionic conductivity, σ_0 is the pre-exponential factor, E_a is the activation energy, T is absolute temperature).

γ decreases, the distribution of relaxation time for charge conduction becomes broader. These results suggests that the phase associated with the low frequency arc is inhomogeneous.

The Arrhenius plots are shown in Fig. 3 for the lithium ion conduction through the lithium iodide composite containing 20 mol % Al_2O_3. The values of activation energy (50.9 kJ mol^{-1}) and lithium ionic conductivity (about 1.0×10^{-6} Ω^{-1} cm^{-1} at 298 K) calculated from the high frequency arc during the cooling cycle are reasonably comparable to the values (48.0 kJ mol^{-1} and 1.2×10^{-6} Ω^{-1} cm^{-1} at 298 K) obtained from total impedance during the heating cycle, indicating that the high frequency arc is assigned to the lithium iodide matrix phase. In contrast, the activation energy (74.0 kJ mol^{-1}) and the lithium ionic conductivity (about 2.0×10^{-8} Ω^{-1} cm^{-1} at 298 K) obtained from the low frequency arc during the cooling cycle are much

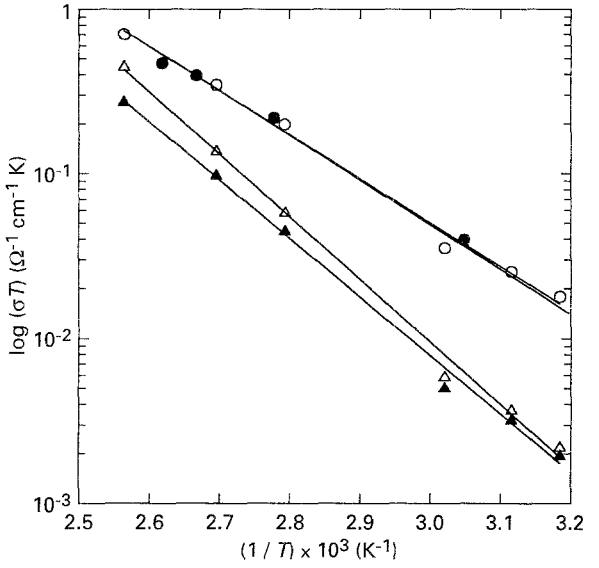

Figure 3 Arrhenius plots obtained from LiI containing 20 mol % Al_2O_3 during the heating and cooling cycles: (○), total impedance during the heating cycle; (△), total impedance during the cooling cycle; (●), high frequency arc during the cooling cycle; (▲), low frequency arc during the cooling cycle. The cooling cycle runs were preceded by holding the specimen at 400 K for 1 h.

higher and lower than those values from the high frequency arc, respectively. This means that the lithium ion conduction through a new phase developed during the holding at 400 K for 1 h and responsible for the low frequency arc is more aggravated than that through the LiI matrix phase.

LiI–Al_2O_3 composite usually contains a small amount of H_2O because of the extremely hygroscopic nature of LiI, despite careful dehydration treatment. Thus, the low frequency arc shown in Fig. 2b may result from H_2O remaining within the LiI–Al_2O_3 composite. The activation energies for lithium ion conduction through three different hydrates of lithium iodide, LiI·H_2O, LiI·$2H_2O$ and LiI·$3H_2O$, were measured to be 66.3, 355.5 and 105.7 kJ mol^{-1}, respectively, and the lithium ion conductivity of LiI·H_2O was given as 2×10^{-7} Ω^{-1} cm^{-1} at 298 K by Rudo *et al.* [5].

The activation energies of LiI·$2H_2O$ and LiI·$3H_2O$ are much higher than the value of the lithium iodide matrix phase. In addition, LiI·$2H_2O$ and LiI·$3H_2O$ phases should be present as a molten state above 353 K according to the phase diagram [5]. Therefore, the two hydrate phases cannot be responsible for the low frequency arc. According to the mixing rule for composite conductor, the effective activation energy measured on average, associated with the low frequency arc, is never determined by the LiI·H_2O phase, providing a relatively lower activation energy and a comparatively higher ionic conductivity.

Let us consider another phase responsible for the low frequency arc. LiOH phase is, as one would expect, energetically more stable than LiI·H_2O phase. In particular, since the LiI·H_2O phase begins to decompose into LiI and H_2O at about 400 K [5], the reaction between metallic lithium electrode and H_2O readily occurs at this temperature. The activation energy for lithium ion conduction through the LiOH phase and the lithium ionic conductivity of that phase were found to be about 82 kJ mol^{-1} and about 1×10^{-13} Ω^{-1} cm^{-1} at 298 K, respectively, by Biefeld and Johnson [13]. Therefore, it is reasonable to consider that the low frequency arc is attributed not to any lithium iodide hydrate phase itself, but to the lithium hydroxide phase distributed inhomogeneously within LiI–Al_2O_3 composite electrolyte near the metallic lithium electrode.

In summary, LiI–Al_2O_3 composites containing 5, 10 and 20 mol % Al_2O_3 showed only a single arc over the frequency range 10^2 to 10^6 Hz at 298 K. The result substantiated the theory that the lithium ionic conductivity is mainly raised by the charge carrier concentration within the LiI matrix. LiI–Al_2O_3 composites showed only a single arc over the frequency range 10^2 to 10^6 Hz during the heating cycle, whereas they presented two seriously merged arcs during the cooling cycle after holding at 400 K for 1 h. The two arcs were reasonably well separated using the CNLS fitting method. The activation energy and ionic conductivity for lithium ion conduction associated with the much depressed low frequency arc (γ = 0.66 to 0.78) were calculated to be

74.0 kJ mol^{-1} and $2.0 \times 10^{-8}\ \Omega^{-1}\ cm^{-1}$, respectively. From the activation energy and the wide dispersion of impedance spectra, it is suggested that lithium hydroxide phase formed inhomogeneously within the LiI–Al_2O_3 composite electrolyte near the lithium electrode at 400 K is responsible for the occurrence of the low frequency additional arc.

Acknowledgement

The receipt of a research grant under the programme Fabrication of Primary Solid-State Battery of LiI/Al_2O_3 1988/1989, from the Ministry of Commerce and Industry (MOCI), Korea, is gratefully acknowledged.

References

1. C. C. LIANG, *J. Electrochem. Soc.* **120** (1973) 1289.
2. J. B. PHIPPS and D. H. WHITMORE, *Solid State Ionics* **9/10** (1983) 123.
3. T. R. JOW and J. B. WAGNER, Jr, *J. Electrochem. Soc.* **126** (1979) 1963.
4. S. PACK, B. OWENS and J. B. WAGNER, Jr, *ibid.* **127** (1980) 2177.
5. K. RUDO, P. HARTWIG and W. WEPPNER, *Revue Chim. Minerale* **17** (1980) 420.
6. N. BONANOS, B. C. H. STEELE, E. P. BUTTLER, W. B. JOHNSON, W. L. WORRELL, D. D. MACDONALD and M. C. H. McKUBRE, in "Impedance spectroscopy", edited by J. R. Macdonald (John Wiley & Sons, New York, 1987) p. 191.
7. C. C. LIANG, A. V. JOSHI and N. E. HAMILTON, *J. Appl. Electrochem.* **8** (1978) 445.
8. T. R. JOW and C. C. LIANG, *J. Electrochem. Soc.* **130** (1983) 737.
9. D. BRAILSFORD, *Solid State Ionics* **21** (1986) 159.
10. J. R. MACDONALD, J. SCHOOMAN and A. P. LEHNEN, *J. Electroanal. Chem.* **131** (1982) 77.
11. G. W. WALTER, D. N. NGUYEN and M. A. D. MADURASINGHE, *Electrochim. Acta* **37** (1992) 245.
12. K. S. COLE and R. H. COLE, *J. Chem. Phys.* **9** (1941) 341.
13. R. M. BIEFELD and R. T. JOHNSON, Jr, *J. Electrochem. Soc.* **126** (1979) 1.

Received 20 September
and accepted 21 October 1993